Role of Network Connectivity on the Mechanical Properties of Highly Cross-Linked Polymers

Mesfin Tsige,* Christian D. Lorenz, and Mark J. Stevens

Sandia National Laboratories, Albuquerque, New Mexico 87185

Received May 11, 2004; Revised Manuscript Received August 20, 2004

ABSTRACT: The effects of mixed functionality and degree of curing on the stress−strain behavior of highly cross-linked polymer networks are studied using molecular dynamics simulations. The networks are made dynamically in a manner similar to epoxy network formation, and the average functionality of the cross-linker, f_{av}, is systematically varied from 3 to 6 by mixing cross-linkers with functionalities $f =$ 3, 4, and 6. Stress−strain curves are determined for each system from tensile pull simulations. The range of strain of the plateau region (R_P) in the stress−strain curve, failure strain (ϵ_f), and failure stress (σ_f) for fully cured networks are found to have a power law dependence on f_{av} as $\sim f_{av}^{\alpha}$. For R_P and ϵ_f, α is determined to be −1.22(3) and −1.26(4), respectively. The failure strain is equal to the strain needed to make taut the maximum of the minimal paths through the network connecting the two solid surfaces. The failure stress, however, shows two distinct regions. For $f_{av}^{\alpha} \leq 4$, σ_f increases with increase in f_{av} and $\alpha = 1.22(5)$. In this f_{av} regime, the work to failure is constant. For $f_{av}^{\alpha} \geq 4$, the systems fail interfacially, σ_f becomes a constant, and work to failure decreases with f_{av}. These mechanical properties are also found to depend on the degree of curing. With decrease in percentage of curing, failure stress decreases and failure strain increases. The mode of failure changes from interfacial to bulk.

1. Introduction

Cross-linked polymer networks such as epoxy resins have demonstrated excellent mechanical and chemical properties and thus are widely used as structural adhesives in a variety of applications such as optical communication devices, coatings, and packaging industries.[1−5] Epoxy thermoset networks are chemically cured networks based on the reaction between a resin (e.g., diglycidyl ether of bisphenol A) and a cross-linker. Because of the wide variety of cross-linkers and resins available, it is necessary to determine how the molecular architecture affects the mechanical properties of these systems. In this work highly cross-linked networks, which are typical adhesive materials, are studied. The network structure of these materials depend on the functionality of the cross-linker. The effect of cross-linker functionality on the fracture toughness of epoxy networks has been studied in bulk experiments.[2] However, the fracture mechanics at interfaces is different from the bulk, and it is difficult to measure mechanical properties at interfaces. In this work, to understand mechanical properties at both the interface and bulk, we use molecular dynamics (MD) simulations to study the effect of mixed functionalities and degree of curing on the stress−strain behavior of model epoxy systems.

Recent developments in large-scale molecular simulation techniques provide a tool for studying highly cross-linked polymer networks. The simple coarse-grained bead−spring model has been used for a while to study bulk polymer melts and networks.[6,7] We have recently used the model for highly cross-linked polymer systems and showed that it qualitatively models the essential characteristics of these systems.[8−11] In a preceding paper,[10] which will be referred to hereafter as paper I, we calculated stress−strain curves for networks cured with cross-linkers of a given functionality *f*. The cross-linker functionality was found to be an important network characteristic parameter. Higher functionality yielded higher failure stress but a lower failure strain. To further our understanding, it is important to study the effect of mixing different functional cross-linkers on mechanical properties of these networks. One major technological advantage of this is to tailor properties for specific applications.[2,12,13] Here we present molecular dynamics simulations of mixed functional networks bonded to a rigid surface. Using MD simulations, we can directly determine the local structure of the adhesive as a function of deformation and simultaneously calculate the stress−strain curves.

As in our previous studies we have started from a coarse-grained model to simplify the task as much as possible, yet maintain the essential physical characteristics. The main goal of this work was to understand the effects of mixed functionality on the mechanical properties of highly cross-linked networks. These networks were produced by varying the ratios between the different functional cross-linkers in the mixture while maintaining the stoichiometry of the system. Related to mixed functionality is variation of the degree of curing. Any system less than fully cured will have a mixture of functionalities. We also directly studied the influence of the degree of curing on mechanical properties of the interface for systems with a single cross-linker functionality.

This paper is organized as follows. In section 2 the bead−spring model and details of the simulation method used to form and strain the networks are presented. The mechanical properties and failure mechanism of networks cross-linked with mixed functionals are reported in section 3.1. The effect of degree of curing on the mechanical properties is discussed in detail in section 3.2. Finally, conclusions are presented in section 4.

* Corresponding author: e-mail mtsige@sandia.gov.

10.1021/ma049074b CCC: $27.50
Published on Web 10/01/2004

2. Simulation Method

The basic model of highly cross-linked polymer networks is the same as used in earlier work.[8−10] The polymers are treated as bead−spring molecules. The initial system is a mixture of two-bead and three-bead molecules. The two-bead molecules represent the resin strands, while the three-bead molecules represent a two-bead strand already bonded to an *f*-fold functional cross-linker bead. The number of cross-linkers in the system is determined by stoichiometry.

In this work, the beads interact through the standard Lennard-Jones (LJ) 6−12 potential[7]

$$U_{\mathrm{LJ}}(r) = 4u_0\left[\left(\frac{d}{r}\right)^{12} - \left(\frac{d}{r}\right)^{6}\right] \tag{1}$$

with a cutoff at a separation distance of $r = 2.5d$. In eq 1, u_0 and d represent the LJ energy and the diameter of a bead, respectively. All of the beads in these systems have been given identical LJ parameters. The bond potential which allows bond breaking while preserving force continuity is the same as used in paper I.

Initially, the two-bead and three-bead molecules (approximately 90 000 beads) are placed randomly between two solid walls. The simulation cell dimensions are 58.4d × 28.9d × 60.7d. The wall is described in paper I. To place all of the beads into the simulation box at a desired liquid density $\rho_l = 0.8d^{-3}$, the beads are allowed to overlap one another. The overlap is then removed from the randomly placed molecules by applying a cosine potential

$$U_{\mathrm{soft}} = A + A\cos\left(\frac{\pi r}{r_0}\right) \tag{2}$$

where $r_0 = 2^{1/6}d$ is the cutoff. The amplitude A is increased from 0.0 to 60.0 over the span of 1000 time steps. Then the liquid system is equilibrated at $T_l = 1.1u_0/k_{\mathrm{B}}$ for 100 000 time steps to remove artifacts of the initial state.

In epoxies, the liquid mixture of cross-linker molecules and resin molecules is cross-linked dynamically. In the simulations, the mixture of two-bead and three-bead molecules is also dynamically cross-linked. In this work, we focus on systems with mixed cross-linker functionality and on systems with different degrees of curing. For the mixed cases, we simulated binary and ternary mixtures of $f = 3$, 4, and 6 cross-linkers. The network is dynamically formed during a constant temperature simulation using a two-stage curing process, in which bonds are formed when the separation between a cross-linker and a strand end or wall particle is less than 1.3d. During the first curing stage, cross-linkers are bonded to the walls. In this study, only one bond per cross-linker to a surface was allowed. In the second stage, the cross-linkers are bonded to strands until a desired percentage of all possible bonds are formed. These simulations were run until at least 96% of the possible bonds were formed. For studying systems of variable curing, the cure simulation was simply stopped at the desired percentage. Throughout the cross-linking process, zero load is maintained on the surfaces which allows the volume to adjust to the curing. Note that in paper I zero load was maintained only during bonding to the walls. Afterward, the temperature is reduced below the glass transition temperature ($T_{\mathrm{g}} = 0.5u_0$) to $0.3u_0$. The top surface moves under a small load so that the density can increase due to the drop in temperature.

The stress−strain behavior of these systems are obtained by conducting tensile strain simulations. In these simulations, the top wall is moved at a constant rate $v_z = 0.02d/\tau$ in the z-direction away from the rigid bottom wall. Previous simulations have shown this to be a reasonable value.[8−10] The stress in our simulations is computed as the resultant force on the wall per unit area. In our simulations the bead size corresponds to about $d \approx 1$ nm based on the size of epoxy constituent molecules. Based on this mapping the systems have a height of about 60 nm. Estimates of the plastic zone size at a crack tip in unfilled brittle epoxies give values of about 10 μm, which is much larger than our system size and for that matter not feasible for molecular level simulations. The simulations thus treat the region at or near the crack tip. In this region strains and possibly stresses are much larger than the macroscopic measured values.

3. Results and Discussion

3.1. Mixed Functionalities. We have studied four different sets of mixed functional networks and will be named hereafter as follows: (1) 3:4 functional mixture for networks cured with $f = 3$ and 4 and, similarly, (2) 3:6, (3) 4:6, and (4) 3:4:6 functional mixtures. The fraction of each functionality in the mixture was varied from 0 to 1, and the details of the simulated systems and their properties are summarized in Tables 1 and 2. The average cross-linker functionality (f_{av}) for each system was calculated from stoichiometry using the following equation

$$f_{\mathrm{av}} = \sum_{f=3}^{6} \phi_{\mathrm{f}} f \tag{3}$$

where ϕ_{f} is mole fraction of cross-linkers of functionality f and $\sum\phi_{\mathrm{f}} = 1$. The values of f_{av} for the networks are also given in Tables 1 and 2.

Figure 1 shows the stress−strain behavior of 3:4, 3:6, and 4:6 mixed functional networks. All the systems

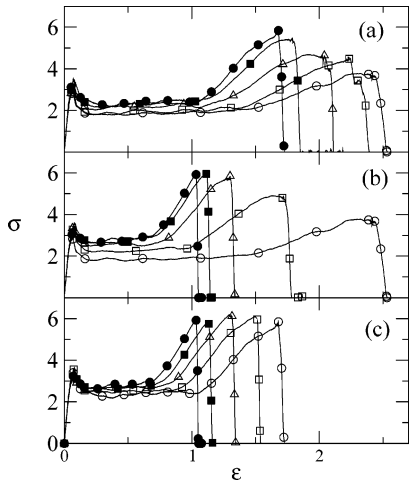

Figure 1. Tensile stress−strain curves for functional mixtures of (a) 3:4, (b) 3:6, and (c) 4:6. The points represent the fraction of the smaller functionality in the mixture: 100% (circles), 75% (open squares), 50% (triangles), 25% (closed squares), and 0% (closed circles).

Table 1. Summary of 3:4 and 3:6 Functional Mixtures and Their Network Properties[a]

3:4-functional mixture						3:6-functional mixture					
ϕ_3	ϕ_4	f_{av}	σ_f	ϵ_f	$\epsilon_{max\ P}$	ϕ_3	ϕ_6	f_{av}	σ_f	ϵ_f	$\epsilon_{max\ P}$
1.00	0.00	3.00	3.9	2.48	2.36	0.95	0.05	3.15	4.5	2.34	2.19
0.90	0.10	3.10	4.3	2.41	2.39	0.90	0.10	3.30	4.7	2.18	2.12
0.85	0.15	3.15	4.5	2.31	2.26	0.85	0.15	3.45	4.9	2.06	1.93
0.75	0.25	3.25	4.6	2.15	2.11	0.75	0.25	3.75	5.4	1.80	1.79
0.60	0.40	3.40	4.7	2.11	2.00	0.67	0.33	3.99	5.9	1.62	1.58
0.50	0.50	3.50	4.8	2.07	1.96	0.60	0.40	4.20	5.9	1.51	1.47
0.40	0.60	3.60	5.1	1.93	1.89	0.50	0.50	4.50	6.0	1.39	1.36
0.25	0.75	3.75	5.3	1.82	1.81	0.40	0.60	4.80	5.9	1.24	1.23
0.15	0.85	3.85	5.7	1.73	1.73	0.25	0.75	5.25	6.0	1.16	1.15
0.00	1.0	4.00	5.9	1.70	1.68	0.15	0.85	5.55	6.0	1.07	1.06

[a] ϕ_i is the fraction of functionality i in the mixture, f_{av} is average cross-linker functionality, σ_f is failure stress, ϵ_f is failure strain, and $\epsilon_{max\ P}$ is the maximum strain required to make the minimal path taut.

Table 2. Summary of 4:6 and 3:4:6 Functional Mixtures and Their Network Properties

4:6-functional mixture						3:4:6-functional mixture						
ϕ_4	ϕ_6	f_{av}	σ_f	ϵ_f	$\epsilon_{max\ P}$	ϕ_3	ϕ_4	ϕ_6	f_{av}	σ_f	ϵ_f	$\epsilon_{max\ P}$
0.85	0.15	4.30	5.9	1.54	1.52	0.80	0.10	0.10	3.40	4.8	2.08	2.04
0.75	0.25	4.50	6.0	1.43	1.42	0.60	0.25	0.15	3.70	5.2	2.00	1.91
0.60	0.40	4.80	5.9	1.33	1.32	0.50	0.25	0.25	4.00	5.9	1.69	1.61
0.50	0.50	5.00	6.0	1.26	1.25	0.34	0.34	0.32	4.30	5.9	1.46	1.41
0.40	0.60	5.20	6.0	1.19	1.18	0.25	0.25	0.50	4.75	6.0	1.24	1.23
0.25	0.75	5.50	5.9	1.13	1.11	0.15	0.15	0.70	5.25	6.0	1.21	1.18
0.00	1.0	6.00	5.9	1.05	1.04	0.10	0.10	0.80	5.50	6.0	1.14	1.12

show a qualitatively similar stress−strain behavior. The initial linear elastic response is followed by yielding. A plateau region exists where the stress is constant for a wide range of strains. The plateau region is where strands are pulled taut. Once the bonds are taut, the stress rises at larger strains due to bond stretching. Bonds break in this region, and finally the stress drops as the system fails. Note that since zero load was maintained on the walls during curing, there is a peak at the yield point that does not appear in paper I. In applying a load during cure, a more compact structure occurs. Consequently, the stress to yield the structure is larger, and the peak in the stress occurs.

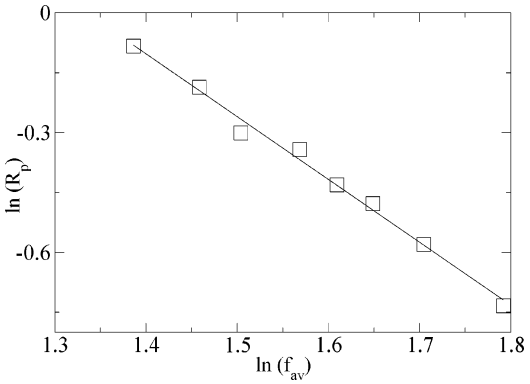

Figure 2. Dependence of the range of the plateau region on average functionality of a cross-linker for the 4:6 functional mixture case. The solid line is a linear fit to the data and has a slope of -1.22 ± 0.03.

As discussed in detail in paper I, the yield stress, the range of the plateau region, and the failure strain strongly depend on the functionality of the cross-linker as can be seen in Figure 1. The yield strain, however, is independent of f_{av} and occurs at a strain of about 0.1, where the maximum in the LJ force to separate neighboring beads is reached. This is because for strains less than 0.1, the response of the system was found to be independent of the bonding nature of the system and depend solely on the nonbond intermolecular interactions.[14]

Beyond the yield point, a plateau region of approximately constant stress occurs as the strands in the network are being pulled taut, but the bonds are not stretched. The range of strain of the plateau region (R_P) decreases with increase in f_{av}. As described in detail in paper I, strands are more extended (less compact) for larger f_{av}. Thus, the strain necessary to make the strands taut is less, and R_P decreases with f_{av}. In Figure 2, R_P, which is defined as the difference between the strain at which the stress begins to rise due to bond stretching and the yield strain, vs f_{av} is shown in a log−log plot for the 4:6 functional mixture. The solid line is a linear fit to the data and has a slope of -1.22 ± 0.03. A similar inverse power law dependence of R_P on f_{av} is observed for the other cases. Note that the stress value of the plateau region shows a slight increase with increase in f_{av}. The increase is specially noticeable in Figure 1b.

The dependence of failure stress (the peak in the stress−strain curve just before failure) on f_{av} is not

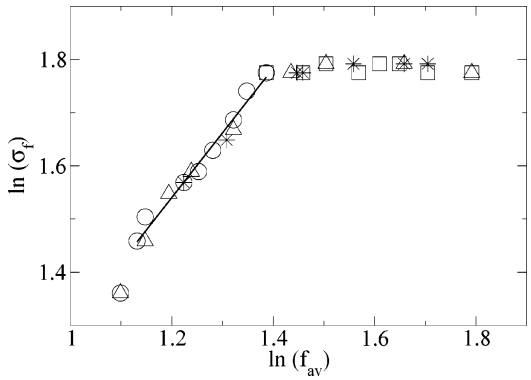

Figure 3. Plot of the log of failure stress vs log of f_{av} for mixtures of 3:4 (circles), 3:6 (triangles), 4:6 (squares), and 3:4:6 (*). The solid line is a linear fit with slope 1.22 ± 0.06.

immediately clear from Figure 1. Figure 3 illustrates the relation between failure stress and f_{av} for the four different sets. Independent of the mixture, the failure stress increases with f_{av} up to $f_{av} = 4$ ($\ln f_{av} \simeq 1.4$) and

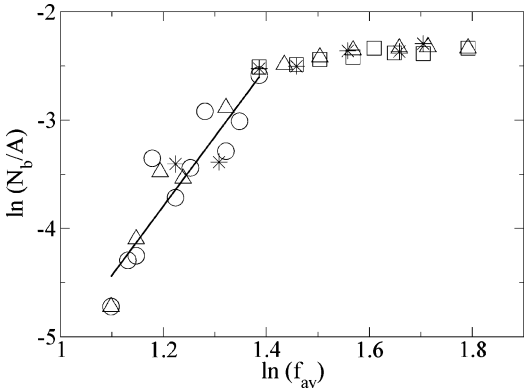

Figure 4. Logarithmic plot of number of broken bonds per unit area on the walls vs f_{av}. The solid line is a linear fit for $f_{av} \leq 4$.

then stays constant. The value for the pure $f = 3$ ($\ln f \approx 1.1$) system appears to be distinct from $f_{av} > 3.0$. The solid line in the figure is a linear fit for the range $3.0 < f_{av} \leq 4.0$ and has a slope of 1.22 ± 0.05.

The reason for the different regions for σ_f as a function of f_{av} can be found by analyzing where and how the systems fail. Examination of configurations shows that $f = 3$ fails cohesively while $f_{av} \geq 4$ fails interfacially. For $3.0 < f_{av} \leq 4$ the system exhibits a mixture of cohesive and adhesive failure. $f = 3$ fails in part by developing a number of large voids within the bulk. For $f = 3$, the network connectivity is relatively low. Neighboring parts of the system are unconnected. Upon the site strain, these parts are pulled apart, forming voids. No bonds break in this case. The number and size of these voids decrease as we increase f_{av} and disappear as we approach $f_{av} = 4$. As f_{av} increases from 3, more and more of the network is well connected. This reduces the size and number of voids that can form.

To understand why $f = 3$ fails cohesively, we compare a plane at an arbitrary z position and the plane at the interface. In the case of $f = 3$, cross-linkers on average have either one bond with a component in the $+z$ direction and two bonds with a component in the $-z$ direction or vice versa. Thus, there is a surface in the bulk along which only one bond per cross-linker needs to be broken to fracture the system. Locally, this surface is equally weak as the interface. But, the interface has a slightly larger density and thus is stronger. Consequently, the bonds in the bulk break preferentially, and the system fails cohesively.

As f_{av} increases, the number of bonds per cross-linker in the bulk with components in either z-direction is greater than at the interface. For $f_{av} = 4$, since cross-linkers in the bulk have an average of two bonds with a component in the $+z$ direction and two bonds with a component in the $-z$ direction, the areal bond density is lower at the interface than any where in the bulk. Thus, fewer bonds at the interface must support the load. The interfacial bonds consequently stretch and break first. Increasing f_{av} beyond 4 has no effect on the failure stress since the location of failure has shifted to the interface whose structure does not depend on f_{av}.

To confirm this point, we counted the number of broken bonds per unit area at the walls, N_b/A (Figure 4). In general, N_b/A increases until $f_{av} = 4$ and then stays almost constant. The scatter is greater than in Figure 3, but the behavior is in accordance with the picture described above.

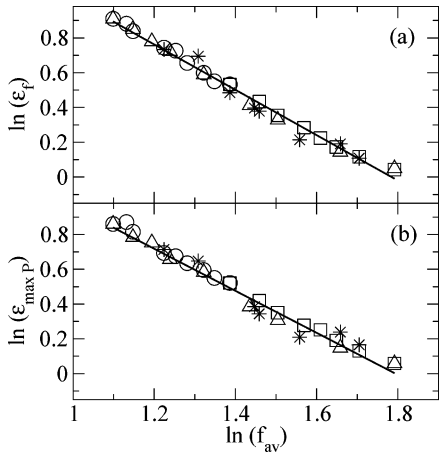

Figure 5. Dependence of (a) failure strain and (b) maximum minimal path, $\epsilon_{max\,P}$, on f_{av} for the four different functional mixture cases: 3:4 (circles), 3:6 (triangles), 4:6 (squares), and 3:4:6 (*). The solid line is a linear fit to the data and has a slope of -1.26 ± 0.04 and -1.22 ± 0.03, respectively.

The dependence of failure strain, ϵ_f, on f_{av} for all the systems studied is shown in a log−log plot in Figure 5a. The failure strain is defined as the strain at the midpoint between the failure stress (peak) and zero stress after this peak. All the four different sets show that with increasing f_{av} there is a decrease in the failure strain. In Figure 5a we see that components of the mixed cross-linkers have little effect on the failure strain. The solid line is a linear fit to the data and has a slope of -1.26 ± 0.04, which is within uncertainty the same exponent found for σ_f.

In paper I, we have shown that the failure strain and the network structure are directly related. The maximum of the minimal path length of the network has been directly related to the failure strain of the system. For a site on the bottom surface to which the network is bonded, there are many possible paths through the polymer network to the top surface. The shortest path defines the minimal path length P for that particular bottom surface bonding site. There is a set of P for a given system, one for each bonding site at the bottom surface. P has been calculated using Dijkstra's method[15] for all bonding sites on the bottom surface and is converted into a strain via the relation $\epsilon_P = (P - L_z)/L_z$, where L_z is the unstrained separation distance between the surfaces. For $\epsilon > \epsilon_P$, some bond within the given minimal path must stretch or break. The simulation shows that the strain for the maximum of the minimal paths, ϵ_{maxP}, given in Tables 1 and 2 is generally in good agreement with ϵ_f. $\epsilon_{max\,P}$ is slightly smaller than ϵ_f (<10%) since additional strain is required to stretch bonds to the breaking point.

Figure 5b is a plot of the maximum of the minimal paths vs f_{av} for the four different cases. As expected, the dependence is similar to that of Figure 5a. The solid line is a linear fit to the data and has a slope of -1.22 ± 0.03, which is within the uncertainty of the exponent found for ϵ_f in Figure 5a. The similarity in the scaling of the minimal paths and ϵ_f shows that the minimal path is the network characteristic which determines ϵ_f.

When we examine the combined results for R_P, σ_f, ϵ_f, and $\epsilon_{max\,P}$, we find a consistent, if unexpected, set of results. All show a power law dependence on f_{av} as $f_{av}^{\pm\alpha}$ with almost the same scaling factor of $\alpha \approx 5/4$. Though this observed correlation between the different mechanical properties and f_{av} is encouraging in terms of

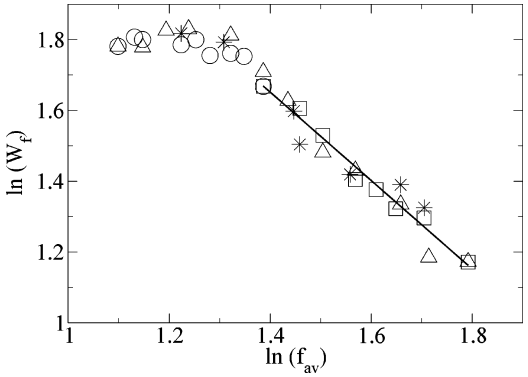

Figure 6. Plot of the log of work to failure vs log of f_{av} for mixtures of 3:4 (circles), 3:6 (triangles), 4:6 (squares), and 3:4:6 (*). The solid line is a linear fit for $f_{av} \geq 4$ and has a slope of -1.23 ± 0.07.

quantitatively understanding the fracture behavior of the networks, it should be emphasized that this correlation may be specific to our model. For instance, manipulating the interaction parameters between the different beads may affect P and ϵ_f and may result in two different scaling factors. Therefore, further study of this correlation should be performed and will be considered in our future work.

The scaling results of σ_f and ϵ_f suggest that $\sigma_f\epsilon_f =$ constant for $f_{av} \leq 4$. The product of σ and ϵ is related to the work to failure (W_f). In Figure 6 we plot W_f, which is the area under the stress−strain curve, as a function of f_{av}. The work to failure is constant for $f_{av} < 4$, implying that the cohesive to adhesive transition in this regime takes place at a constant work to failure. W_f can be divided into the sum of two parts of integral of the stress−strain plot. One part is the area under the plateau region. This decreases with f_{av} since R_P decreases. The second part is the area under the curve from the final strain value of the plateau region to ϵ_f. This increases with f_{av} for $f_{av} \leq 4$. Figure 1a shows that the two components compensate to yield a constant W_f. The solid line in Figure 6 is a linear fit for $f_{av} \geq 4$ and has a slope of -1.235 ± 0.07. In this interfacial failure region, the work to failure scales the same as ϵ_f and R_P since σ_f is a constant. Further investigation of Figure 1c indicates that the second part contributing to W_f is almost a constant for $f_{av} \geq 4$. This is not surprising since for $f_{av} \geq 4$ the majority of the bonds that are stretched and then break are those connected to the walls whose bond density does not depend on f_{av}. Thus, the observed decrease of the work to failure in this region is solely due to the decrease in R_P (range of strain of the plateau region).

Since the simulations are limited to small volumes, there are no direct comparisons to experiment. However, the recent experimental results by Crawford and Lesser[2] on the fracture behavior of epoxy resins for $3.09 \leq f_{av} \leq 4.0$ shows that chemical nature of the curing agents has little effect on the rubbery moduli of the networks in agreement with our simulation result.

3.2. Degree of Curing. The effect of the degree of curing (cross-linking) on the mechanical properties of the networks is shown in Figure 7 for $f = 3$, 4, and 6. For a given f, the number of interfacial bonds is fixed and the degree of curing is varied only within the bulk. In all cases, failure stress decreases while failure strain increases with decrease in percentage of curing. This behavior is similar to the effect observed in the previous

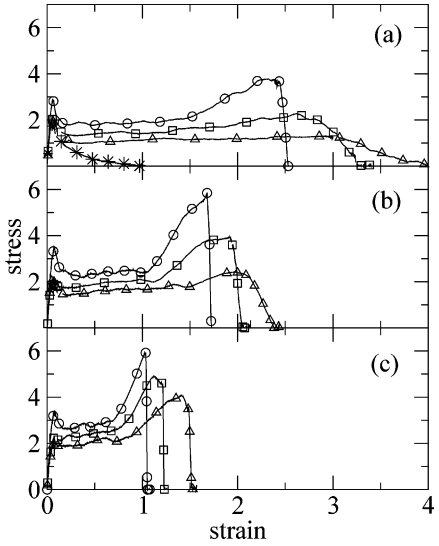

Figure 7. Tensile stress−strain curves for functionalities of (a) 3, (b) 4, and (c) 6. The points represent the percentage of curing: >96% (circles), 85% (squares), 75% (triangles), and 50% (*).

section by changing the functionality of the cross-linker. This similarity is expected since decreasing the degree of curing effectively results in a decrease in the functionality of the cross-linker as described below. Since in our present model, cross-linkers differ only by the number of bonds they can make, curing a system partially will result in cross-linkers of mixed functionalities. For instance, after partially curing a system with cross-linkers of maximum functionality of 4, a given fraction (ϕ_4) of the cross-linkers has made four bonds while the remaining cross-linkers have 1, 2, or 3 bonds, resulting in an average cross-linker functionality of less than 4, but off-stoichiometry. As the percentage of curing further decreases, this average cross-linker functionality decreases. Correspondingly, the failure behavior of the system changes. There is, however, no direct relation between the average cross-linker functionality of the partially cured networks and f_{av} discussed in the previous section due to differences in stoichiometry. In this section, our main objective is to qualitatively understand the effect of curing on the mechanical properties of the networks.

Figure 8 shows snapshots of $f = 3$ and 4 at full curing and 75% curing. The 75% curing system of $f = 4$ fails within the bulk by developing voids in the same way as the fully cross-linked system of $f = 3$, indicating that it is closer to $f = 3$ than $f = 4$ as can be seen also from the stress−strain curves. The 75% cured system of $f = 3$ exhibits a structure similar to crazing in non-cross-linked polymers.[16−18] Note that the decrease in failure stress with decrease in percentage of curing observed in Figure 7 for $f = 4$ and 6 is due to the transition from interfacial to cohesive failure, as shown in Figure 8 for $f = 4$.

Below the percolation threshold there is no cluster within the network that spans from one wall to the other. To determine the percolation threshold value of a given f_{av}, we performed the minimum path calculation on unstrained system at different degrees of curing. The degree of curing below which there is no longer a minimal path from the bottom wall to the top wall is called the percolation threshold. The percolation threshold value was found to depend on f_{av} and is specifically 64% for $f = 3$, 50% for $f = 4$, and 44% for $f = 6$. Within

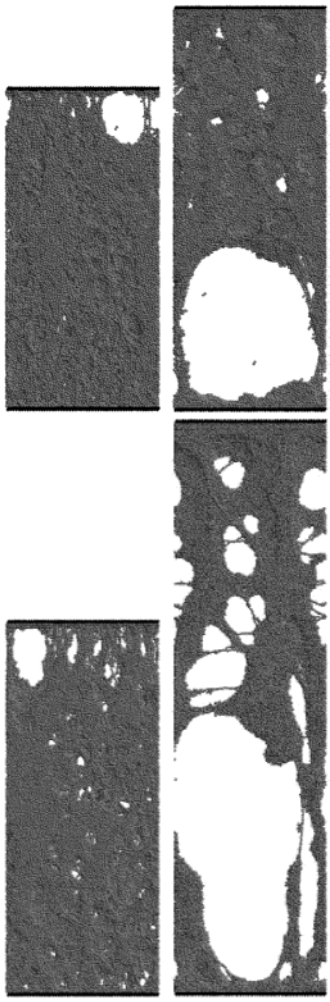

Figure 8. Images before failure: top panel is for $f = 4$, fully cross-linked, and $f = 4$, 75% cross-linked; bottom panel is for $f = 3$, fully cross-linked, and $f = 3$, 75% cross-linked.

the error of the simulation there is no clear dependence of the threshold value on the functionalities that are mixed, but instead tends to depend only on f_{av}.

For degree of curing smaller than the threshold value, the contribution of bonds to stress is negligible as shown in Figure 7a for 50% curing of $f = 3$, and the stress−strain behavior becomes independent of f and is similar to a nonbonded system.[14] In this case, the failure stress becomes the stress required to separate van der Waals surfaces.

4. Conclusions

We used molecular dynamics simulations to study the stress−strain behavior of highly cross-linked polymer networks under tensile pull as the effective functionality of a cross-linker increases. The networks were made dynamically in a manner similar to epoxy network formation in which a cross-linker and resin dynamically react to form the network. The average functionality of the cross-linker, f_{av}, was varied from 3 to 6 by mixing cross-linkers of $f = 3$, 4, and 6. The fraction of each f in the mixture was varied from 0 to 1 while maintaining the stoichiometry of the system. The stress−strain behavior was studied for each system. We found that only the average functionality of the system f_{av} and not the type of the components of the mixed cross-linkers that controls the mechanical properties of the system.

The dependence of the stress−strain curves and the location of failure on the cross-linker functionality have been discussed in detail. The range of the plateau region in the stress−strain curve, failure strain, and failure stress were found to show power law dependence on f_{av}. The plateau region where strands are pulled taut was found to decrease with increase in f_{av} as $R_p \sim f_{av}^{-1.22}$. Also, the failure strain (ϵ_f) dropped as $\epsilon_f \sim f_{av}^{-1.26}$. The difference between the two exponents is within the error of the simulation. The similarity between the two is not surprising since both reflect the compactness of the strands in the system. Our simulation indicated that the failure strain can be predicted a priori from the network structure. The failure strain was found to be equal to the strain needed to make taut the maximum of the minimal paths through the network connecting the two walls.

The failure stress (σ_f), on the other hand, showed two distinct regions. For $f_{av} \leq 4$, the failure stress increased as $\sigma_f \sim f_{av}^{1.22}$. In this region, increasing f_{av} resulted in a transition from cohesive to adhesive failure. Examination of configurations also showed that $f = 3$ failed by developing a number of large voids within the bulk, and the number and size of these voids decreased as f_{av} increased and disappeared when f_{av} approached 4. For $f_{av} \geq 4$, the system failed interfacially and σ_f became a constant. This is because the location of failure has shifted to the interface, and further increase in f_{av} has no effect on σ_f since the bonds that had to be stretched and broken are the ones connected to the walls.

For $f_{av} \leq 4$, the scaling of σ_f is f_{av}^{α} and ϵ_f is $f_{av}^{-\alpha}$, where $\alpha \approx {}^5/_4$. Furthermore, the work to failure in this regime is constant; for $3 < f_{av} \leq 4$, the system undergoes a transition from cohesive to adhesive failure. The result seems significant but needs to be studied further to determine its generality. The work to failure decreases for $4 \leq f_{av} \leq 6$ due to a smaller plateau regime in which the network strands are pulled taut.

The dependence of the mechanical properties of networks made with single functional cross-linkers ($f = 3$, 4, or 6) on the degree of curing has also been calculated. In all cases, we observed that with decrease in percentage of curing failure stress decreased and failure strain increased. This behavior has been explained in terms of variation in cross-linker functionality due to a change in curing condition. As the percentage of curing decreased, the mode of failure changed from adhesive to cohesive. Below the percolation threshold the bond contribution to stress is negligible. The percolation threshold value was found to decrease with increase in f.

Acknowledgment. This work was supported by the DOE under Contract DE-AC04-94AL8500. Sandia is a multiprogram laboratory operated by Sandia Corp., a Lockheed Martin Company, for the DOE.

References and Notes

(1) Meyer, F.; Sanz, G.; Eceiza, A.; Mondragon, I.; Mijovic, J. *Polymer* **1995**, *36*, 1407.
(2) Crawford, E.; Lesser, A. J. *J. Polym. Sci., Part B* **1998**, *36*, 1371.
(3) Kannurpatti, A. R.; Anseth, J. W.; Bowman, C. N. *Polymer* **1998**, *39*, 2507.
(4) Mustaja, F.; Bicu, I. *J. Appl. Polym. Sci.* **2000**, *77*, 2430.
(5) Paul, G. K.; Ramakrishnan, S. *Macromol. Chem. Phys.* **2001**, *202*, 2872.

(6) Binder, K., Ed.; *Monte Carlo and Molecular Dynamics Simulations in Polymer Science;* Oxford: New York, 1995.
(7) Kremer, K.; Grest, G. In *Monte Carlo and Molecular Dynamics Simulations in Polymer Science*; Binder, K., Ed.; Oxford: New York, 1995; Chapter 4, pp 194−271.
(8) Stevens, M. J. *Macromolecules* **2001**, *34*, 1411.
(9) Stevens, M. J. *Macromolecules* **2001**, *34*, 2710.
(10) Tsige, M.; Stevens, M. J. *Macromolecules* **2004**, *37*, 630.
(11) Lorenz, C. D.; Stevens, M. J.; Wool, R. P. *J. Polym. Sci., Part B: Polym. Phys.* **2004**, *42*, 3333.
(12) de Nograro, F. F.; Liano-Ponte, R.; Mondragon, I. *Polymer* **1996**, *37*, 1589.
(13) Lesser, A. J.; Crawford, E. *J. Appl. Polym. Sci.* **1997**, *66*, 387.
(14) Lorenz, C. D.; Stevens, M. J. *Phys. Rev. E* **2003**, *68*, 021802.
(15) Hu, T. *Combinatorial Algorithms;* Addison-Wesley: Reading, MA, 1982.
(16) Baljon, A. R. C.; Robbins, M. O. *Macromolecules* **2001**, *34*, 4200.
(17) Rottler, J.; Barsky, S.; Robbins, M. O. *Phys. Rev. Lett.* **2002**, *89*, 148304.
(18) Sides, S. W.; Grest, G. S.; Stevens, M. J.; Plimpton, S. J. *J. Polym. Sci., Part B* **2003**, *42*, 199.

MA049074B